Appl. Phys. B 88, 373–377 (2007)
DOI: 10.1007/s00340-007-2721-8

Applied Physics B
Lasers and Optics

H. KRONEMAYER[1,✉]
P. IFEACHO[1]
C. HECHT[1]
T. DREIER[1]
H. WIGGERS[1,2]
C. SCHULZ[1,2]

Gas-temperature imaging in a low-pressure flame reactor for nano-particle synthesis with multi-line NO-LIF thermometry

[1] IVG, Universität Duisburg-Essen, Lotharstr. 1, 47057 Duisburg, Germany
[2] CeNIDE, Center for Nanointegration Duisburg-Essen, 47057 Duisburg, Germany

Received: 13 March 2007/Revised version: 10 May 2007
Published online: 27 June 2007 • © Springer-Verlag 2007

ABSTRACT Multi-line NO-LIF temperature imaging was applied to measure two-dimensional gas-temperature fields in a low-pressure, premixed flat-flame nano-particle generator during nano-particles synthesis. It was the first time that this calibration-free technique was applied in a low-pressure combustion system. The laser fluence was limited to 4 kW/cm^2 in order to avoid saturation of the LIF signal, which influences the temperature results. While minimizing the elastically scattered light, the efficiency of the LIF detection system improved. This enables measurements with low tracer concentrations that do not influence the nano-particle generation process or the flame chemistry. An optimized scan range for excitation spectra was applied to measure flame temperatures between 600 and 1500 K in a 175×50 mm^2 field with an accuracy of $\pm 2\%$. It was found that the TiO_2 nano-particle generation process does not influence the flame temperature under typical operating conditions. Pressure effects on the temperature distribution were investigated. The data is required for the simulation of nano-particle formation based on kinetic modeling.

PACS 07.20.Dt; 42.62.Fi; 61.46.Df

1 Introduction

Low-pressure premixed flames are a promising route for the synthesis of nano-sized semi-conducting metal-oxide particles. Materials including SnO_2, TiO_2 and ZnO are widely used for gas-sensing devices, photocatalysis and (opto)electronic devices. The temperature-time history of the nano-particle formation within the flame is an important factor that influences particle size, morphology and crystallinity. Therefore, detailed information concerning the gas-phase temperature distribution within the reaction chamber is of specific interest [1]. The flame temperature must be known in order to numerically simulate nano-particle formation based on kinetic modeling. It depends on the fuel/air ratio, the dilution by inert gases, the precursor (i.e., metal-organic species carrying the desired metal atoms) and the total pressure. It also varies with the thermal management of the reactor, e.g., a cooled sinter matrix at the gas inlet and cooling at the reactor walls.

Laser-based imaging techniques have the capability to provide multi-dimensional temperature information without perturbing the investigated system in contrast to sampling techniques or thermocouple measurements. Two-dimensional temperature imaging can be obtained by two-line [2, 3] and multi-line [4] laser-induced fluorescence (LIF) as well as Rayleigh scattering [5] and filtered Rayleigh thermometry [6]. Vibrational and rotational Raman techniques [7] are often limited to line measurements and CARS [8] yields point measurements only. Infrared absorption techniques [9] can provide line-integrated information and therefore do not resolve inhomogeneous temperature distributions.

✉ Fax: +49 203 379 3087, E-mail: helmut.kronemayer@uni-due.de

2 Multi-line NO-LIF thermometry

This LIF thermometry technique is based on the temperature-dependent population of rotational and vibrational energy levels of the nitric oxide (NO) molecule. In contrast to conventional two-color LIF thermometry for gas-temperature imaging [2, 3], the multi-line technique yields absolute temperatures without calibration [10] and can be applied even in systems with strong scattering and fluorescence background as well as in the presence of pressure broadening [4, 11]. It has been used in stoichiometric and sooting flames [4] as well as in spray flames at atmospheric pressure [12, 13] and high-pressure flames up to 6 MPa [11].

The technique is based on the measurement of LIF-excitation spectra of NO, which is added to the fresh gases as a fluorescent tracer. The laser beam is formed to a light sheet, which illuminates a plane in the area of interest. The pulsed laser is tuned over a part of the NO $A - X(0, 0)$ absorption band at 225 nm while individual images are taken with an ICCD camera for each excitation wavelength. The camera is equipped with filters to suppress the detection of elastically scattered light and interference from other laser-excited species. From the resulting stack of pictures (each with the laser tuned to the next wavelength), LIF excitation spectra

can be extracted for each pixel. Simulated spectra are then fitted to the experimental data with an absolute temperature, broad-band background as a baseline and signal intensity as free parameters using LIFSim [14].

In the present experiment, we applied multi-line NO-LIF thermometry for the first time to a low-pressure flame. 200 ppm NO were added to the fresh gases since there is no natural NO production in a $H_2/O_2/Ar$ flame. This small amount avoids disturbance of the lean flame and ensures negligible laser attenuation by NO inside the reactor. The maximum laser attenuation was below 0.2% over the 10 cm cross-section of the apparatus for the strongest absorption feature.

Measurement accuracy

The spectral range of 225.19–225.10 nm (44 406–44 425 cm^{-1}) was chosen for acquiring the excitation spectra. Within this 19 cm^{-1} scan range we find 11 transitions originating from ground state rotational quantum numbers $J'' = 17.5$ to $J'' = 46.5$. This yields optimum temperature sensitivity from ambient temperature up to 2500 K. The transitions are blended into five distinct features, as shown in Fig. 1. It is obvious that the entire shape of the spectrum strongly changes with temperature. This scan range is an improvement compared to previous work [4, 12] because it enables precise measurements in the entire temperature range from 250–2500 K. The smaller range previously used (225.19–225.13 nm) can be applied for either room temperature or temperatures above 1000 K, however, the fitting procedure shows some instabilities in the temperature region from 500–1000 K. Here, LIF signals from higher rotational ground states (at 225.145 and 225.175 nm, marked in Fig. 1) are very weak and interpreted as noise rather than as spectral peaks if the additional peak at 225.12 nm is not present. As a result, the fitted temperature can be approximately 200 K too low.

For each scan, images at 191 wavelength positions, each averaged over 50 laser shots, were taken at equal spectral intervals of 0.1 cm^{-1}. The laser energy was monitored on a shot-by-shot basis and the LIF signal intensity was corrected by linear interpolation. The full data set was acquired within a few minutes. The precision of the temperature measurements is better than ±1%. This was derived from the root mean square (RMS) deviation of the temperature values inside a homogeneous area of each temperature field. Multiple measurements were conducted to ensure reproducibility, which was found to be in the ±1% range if care is taken in stabilizing the thermal management of the reactor. The accuracy of these results is better than ±2%. This is derived from comparisons with thermocouple measurements at 250–350 K and CARS at up to 2200 K [4, 12] with an accuracy of ±0.3% and ±2%, respectively. The uncertainty at elevated temperatures is based on the accuracy of spectroscopic parameters of the NO molecule (±1%) and the assumption of rotational quantum-number independent quenching cross-sections within each vibrational state of the NO A-state (±1%) for the temperature evaluation. Other contributions to the uncertainty such as NO concentration variation or thermal drifts of laboratory equipment are negligible or have been corrected for.

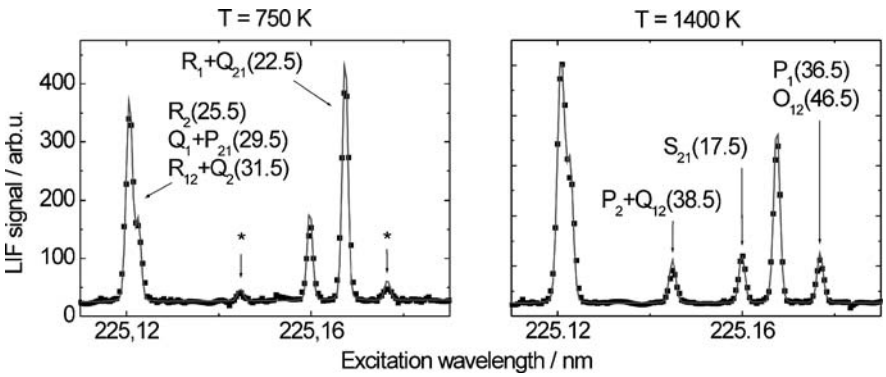

FIGURE 1 Experimental (*symbols*) and the fitted simulated (*lines*) excitation spectra for two different temperatures. The labels show the respective rotational transition in the NO $A - X(0, 0)$ band. Peaks causing instabilities in a previously used scan range are marked in the left graph (∗)

Saturation of the LIF process

Special care was taken to ensure that the excitation energy of the laser was low enough that saturation of the LIF signal did not influence the temperature measurements. At low pressure, collisional quenching of the excited NO molecules is much reduced as compared to atmospheric pressure. Hence, the excited state lifetime is much higher with an increasing probability for stimulated emission and population cycling. Additionally, ground-state rotational energy transfer (RET) is slow at lower collision rates. This limits the thermalization of the population of the rotational states [15]. Accordingly, the ground state rotational level can be easily partially depleted by strong pumping. Both processes cause a deviation from linear signal response on laser intensity and therefore distort the relative intensities measured on the different transitions which in turn influences the temperature evaluation.

We investigated the linearity of the LIF signal of all transitions used in this work. From Fig. 2 it can be seen that a 50×5 mm^2 light sheet can easily saturate the NO transition at 225.12 nm above a power density of 12 kW/cm^2. This feature has the largest transition moment within the spectral range investigated. The light sheet thickness was extended to 10 mm and spectra were taken at a fluence of 4 kW/cm^2, which corresponds to a laser power of 0.4 mJ. The LIF signal was evaluated for different NO concentrations in order to ensure that the camera was working in the linear range.

3 Experimental setup

A tunable, narrowband KrF excimer laser (248 nm, $\Delta\nu \sim 0.3$ cm^{-1}, Lambda Physik EMG 150 TMSC) is frequency-shifted to 225 nm in a Raman cell filled with 5 bar hydrogen, enabling NO excitation in the $A–X$ (0,0) band. The laser beam is expanded in the horizontal direction and compressed in

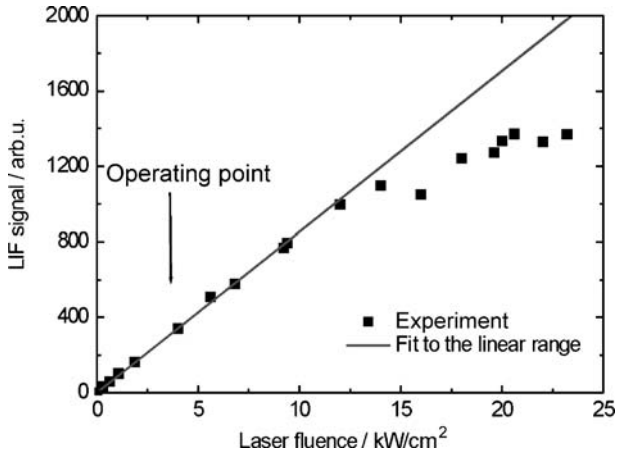

FIGURE 2 NO-LIF intensity as a function of laser fluence at 225.12 nm. The arrow marks the laser fluence used for the temperature measurements

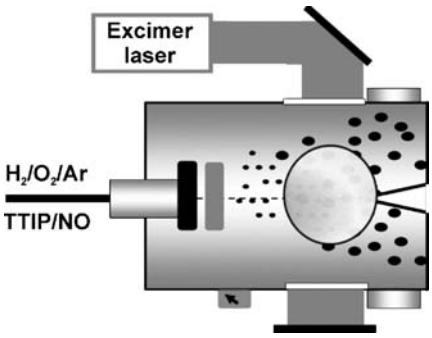

FIGURE 3 Horizontal cut through the flat-flame reactor. Optical access is given through fused silica windows

the vertical direction with two cylindrical lenses $f = 1000$ mm and $f = 300$ mm to form a light sheet of 50×10 mm^2. The LIF signal is recorded with an intensified CCD-camera (LaVision). Elastically-scattered light is suppressed by three long pass filters (230 nm, LayerTec). These edge filters increase the efficiency of the LIF signal detection by one order of magnitude with respect to the Schott UG5 filters used previously [12, 13] while simultaneously improving the rejection of the elastic scattered light by one order of magnitude. This ensures a high signal-to-noise ratio of the excitation spectra even at the low NO concentration of 200 ppm and a low laser fluence of 4 kW/cm^2. The general setup as well as the data evaluation procedure is similar to the one described in [4] and an overview of the reactor is given in Fig. 3.

The flat-flame reactor is described in detail elsewhere [16]. The 36 mm diameter sintered metal-plate burner head is centered in a 300 mm long, horizontally mounted, metal tube with a diameter of 100 mm. Optical access is possible through fused silica windows (50 mm diameter) from three sides. The burner head can be moved horizontally with respect to a reference position, where a skimmer nozzle extends into the reactor to enable online particle size measurements. Hydrogen is used as fuel, oxygen as oxidizer and the mixture is diluted with argon. Typical flow rates for ,e.g., TiO_2 nano-particle production are 600 sccm H_2, 800 sccm O_2, 500 sccm Ar, and 200 ppm of the precursor titanium-tetraisopropoxide (TTIP). The fuel/air ratio of this lean mixture is $\Phi = 0.375$. The flow velocity inside the reactor reaches a few m/s.

4 Results and discussion

The gas-phase temperature field was measured in the $H_2/O_2/Ar/NO/TTIP$ flat flame of the reactor by moving the burner nozzle relative to the window position for five different burner distances. Figure 4 shows the resulting temperature distribution in a 175×50 mm^2 horizontal area of the flame inside the reactor for typical operating conditions at a pressure of 3 kPa. The spatial resolution in the horizontal plane is 1×1 mm^2. The burner head is situated on the left side where the incoming cold premixed fresh gas is located.

Figure 5 shows temperature profiles along the centerline of the reaction chamber for two different conditions. Because of the light sheet thickness of 10 mm, the calculation of the profile includes a 10 mm wide area around the centerline in Fig. 4. At a pressure of 4 kPa, the fresh gas is heated by the flame reactions until a maximum temperature of 1430 K is reached at about a 40 mm distance from the burner surface. Then, the post-flame gas cools down to 750 K at a 175 mm distance. At 3 kPa, which is typically used for TiO_2 nano-

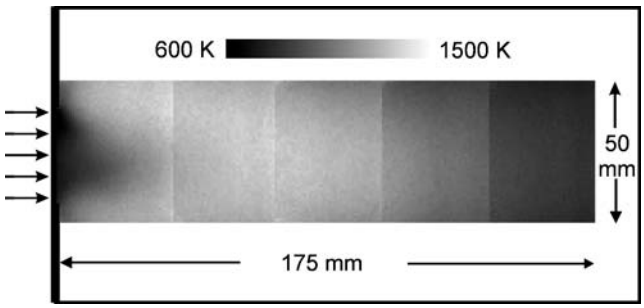

FIGURE 4 Temperature distribution in a horizontal plane inside the reactor

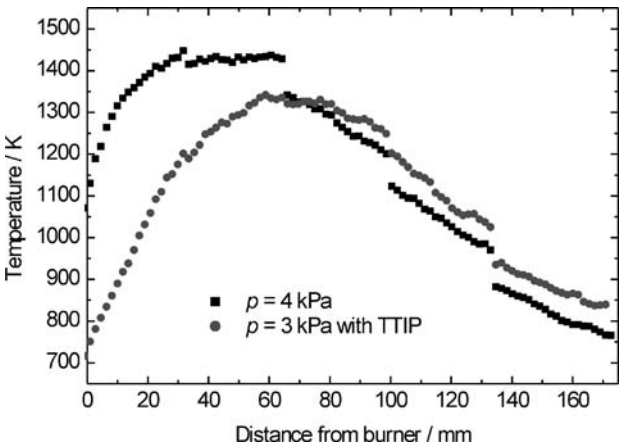

FIGURE 5 Temperature as a function of distance from the burner head for the centerline of the reactor

particle production, the flame front extends to approximately 60 mm into the reaction chamber and the maximum temperature is only 1340 K. After 80 mm distance from the burner head, the burnt gas temperature decreases with a similar rate for both conditions. At lower pressure, the gas temperature at the end of the observation zone is higher since the residence time inside the chamber is shorter and, consequently, the heat transfer to the walls is lower. The measurement procedure by moving the burner head and detecting at the same position can lead to steps in the temperature profile due to an increasing cooling surface between the burner head and the detection position when the burner head is moved away.

Measurements were done with and without the addition of TTIP. It was found that the precursor decomposition, the oxidation of the side chains and the nano-particle generation process does not influence the temperature field within the measurement precision for the titanium system. Additionally, the added NO does not influence the nano-particle generation. The NO-LIF signal strength is identical with and without TTIP addition, even for NO concentrations lower than the TTIP concentration, proving that NO is chemically inert and does not react with TTIP in an, e.g., ligand exchange reaction.

The effect of different NO concentrations on the temperature measurements was investigated. The NO concentration varied between 100 and 1000 ppm while all other parameters were kept constant. No effect on the temperature results could be detected. Furthermore, parameter studies reveal that a richer flame with a fuel/air ratio $\Phi = 0.667$ has a slightly higher maximum temperature than the $\Phi = 0.375$ case.

In stabilized, premixed atmospheric pressure flat flames, the flame front is situated close to the sinter matrix. In this low-pressure flame, the heating zone is stretched as far as 60 mm into the reaction chamber. This enables a homogeneous heating even with highly diluted precursor/gas mixtures and supports the formation of small and only softly agglomerated nano-particles. Particle formation starts instantaneously after the decomposition of the precursors by condensation, growth, coagulation, agglomeration, and sintering. Depending on the time the particles travel through the reaction zone, their size and morphology is different [17].

The multi-line NO-LIF technique is capable of providing temperature data during nano-particle synthesis. Future work will concentrate on the effect of nano-particle synthesis on the temperature inside the reactor for other precursors such as $Fe(CO)_5$, which is used to produce iron oxide particles. The production of metal oxides is a strongly exothermal process that releases heat. Nevertheless, the addition of several 100 ppm of precursor does not significantly influence the overall heat release of the flame. Therefore, no major change in the temperature distribution is expected in the presence of precursors. On the other hand, the precursors may affect the chemical reactions in the flame by influencing the rates of some elementary reactions as known from effective flame quenchers like ferrocene and $Fe(CO)_5$, where gas-phase iron compounds like FeO and FeOH react in catalytic cycles with flame carrier radicals like H and OH. The super equilibrium concentrations of these radicals are reduced towards their equilibrium values, resulting in a reduction in flame speed [18]. This could certainly affect the overall chemical reactions and spatially shift the flame front and, therefore, the temperature distribution.

5 Conclusion

The temperature-time history of the nano-particle formation within a low-pressure, flat-flame reactor influences particle size, morphology and crystallinity. The temperature must be known for numerical simulation of nano-particle formation based on kinetic modeling. Multi-line NO-LIF thermometry is an ideal tool to measure the gas-phase temperature distribution inside a flat flame reactor for nano-particle synthesis. It enables in-situ measurements without perturbing the system. The stable laminar flame allows averaging for flame temperature measurements with an accuracy of $\pm 2\%$. Improvements in the multi-line NO-LIF technique are presented, such as an optimum scan range for the entire temperature range from 250–2500 K. Stray light from particles is suppressed by edge filters that improve the efficiency for fluorescence detection by one order of magnitude with respect to previous work. NO addition does not influence the flame temperature and does not disturb the TiO_2 nano-particle synthesis. It was found that TTIP addition does not influence the temperature distribution inside the reactor at the investigated TTIP concentration of 200 ppm. Parameter studies show the effect of fuel/air ratio and pressure on the temperature field. Gas temperatures between 600 and 1500 K were measured. In low-pressure environments, care must be taken to avoid saturation effects in the LIF process, which can lead to systematic errors in the resulting temperature field. Therefore, temperature measurements were done at a low laser fluence of $4\,kW/cm^2$. Currently, the measured temperature fields are used as a database to develop detailed numerical models for the nano-particle formation process [19]. Future work will concentrate on the chemistry of precursor decomposition and particle formation on the reactor temperature for other precursors such as $Fe(CO)_5$, which is known to be an effective flame quencher.

ACKNOWLEDGEMENTS Funding by the Deutsche Forschungsgemeinschaft (DFG) within SFB445 'Nanopartikel aus der Gasphase' is gratefully acknowledged.

REFERENCES

1 V. Simanzhenkov, P. Ifeacho, H. Wiggers, J. Knipping, P. Roth, J. Nanosci. Nanotechnol. **4**, 157 (2004)
2 M. Tamura, J. Luque, J.E. Harrington, P.A. Berg, G.P. Smith, J.B. Jeffries, D.R. Crosley, Appl. Phys. B **66**, 503 (1998)
3 W.G. Bessler, F. Hildenbrand, C. Schulz, Appl. Opt. **40**, 748 (2001)
4 W.G. Bessler, C. Schulz, Appl. Phys. B **78**, 519 (2004)
5 R.W. Dibble, R.E. Hollenbach, Proc. Combust. Inst. **18**, 1489 (1981)
6 D. Hoffman, K.-U. Münch, A. Leipertz, Opt. Lett. **21**, 525 (1996)
7 K. Kohse-Höinghaus, J.B. Jeffries, *Applied Combustion Diagnostics* (Taylor and Francis, New York, 2002)
8 F. Beyrau, A. Bräuer, T. Seeger, A. Leipertz, Opt. Lett. **29**, 247 (2003)
9 M.G. Allen, Meas. Sci. Technol. **9**, 545 (1998)
10 A.O. Vyrodow, J. Heinze, M. Dillmann, U.E. Meier, W. Stricker, Appl. Phys. B **61**, 409 (1995)
11 T. Lee, W.G. Bessler, H. Kronemayer, C. Schulz, J.B. Jeffries, R.K. Hanson, Appl. Opt. **44**, 6718 (2005)
12 H. Kronemayer, W.G. Bessler, C. Schulz, Appl. Phys. B **81**, 1071 (2005)

13 I. Düwel, H.-W. Ge, H. Kronemayer, R. Dibble, E. Gutheil, C. Schulz, J. Wolfrum, Proc. Combust. Inst. **31**, 2247 (2007)
14 W.G. Bessler, C. Schulz, V. Sick, J.W. Daily, A versatile modeling tool for nitric oxide LIF spectra (http://www.lifsim.com) (3rd Joint meeting of the US sections of The Combustion Institute, Chicago, 2003, PI1)
15 J.W. Daily, W.G. Bessler, C. Schulz, V. Sick, T.B. Settersten, Am. Inst. Aeronaut. Astronaut. J. **43**, 458 (2005)
16 D. Lindackers, M.G.D. Strecker, P. Roth, C. Janzen, S.E. Pratsinsis, Combust. Sci. Technol. **123**, 287 (1997)
17 C. Janzen, P. Roth, Combust. Flame **125**, 1150 (2001)
18 G.T. Linteris, V.R. Katta, F. Takahashi, Combust. Flame **138**, 78 (2004)
19 A. Kowalik, P. Ifeacho, H. Wiggers, C. Schulz, P. Roth, TiO_2 nanoparticle formation in a premixed flame and a plasma reactor, Comparison Between Experiment and Numerical Simulation (European Combustion Meeting (ECM), Chania, Greece, 2007)